O_2 activity in comet 67P/Churyumov-Gerasimenko from observations of electron dissociative excitation by the Rosetta-Alice far-ultraviolet spectrograph

P23G-3519
pfeldman@jhu.edu

Paul D. Feldman (JHU), Jean-Loup Bertaux (LATMOS), Lori M. Feaga (UMd), Brian A. Keeney (SwRI), Matthew M. Knight (UMd), John Noonan (LPL), Joel Wm. Parker (SwRI), Andrew J. Steffl (SwRI), S. Alan Stern (SwRI), Ronald J. Vervack (JHU/APL), and Harold A. Weaver (JHU/APL)

Abstract

We have shown that far-ultraviolet emissions of atomic hydrogen, oxygen, and carbon in the near-nucleus coma of comet 67P/Churyumov-Gerasimenko result primarily from electron impact dissociative excitation of H_2O, CO_2, and O_2. Our initial detection of gas outbursts was based on detection of enhanced atomic oxygen emissions relative to those expected from H_2O or CO_2 and were attributed to electron impact on O_2. This spectral signature of O_2 was also observed in long-term limb observations. Molecular oxygen was first reported to be a significant constituent of the coma from Rosetta/ROSINA mass spectrometer measurements. Of the remote sensing instruments on Rosetta, only the Alice far-ultraviolet spectrograph is capable of measuring spatial and temporal variations of O_2, both from atomic emissions as well as from stellar absorption measurements. Here we report on the detection and use of the far-ultraviolet emissions to estimate the abundance of O_2 relative to H_2O along lines-of-sight above the limb, and its variation over the period February 2015 to January 2016, corresponding to heliocentric distances within ~2.0 AU.

The Alice Spectrograph

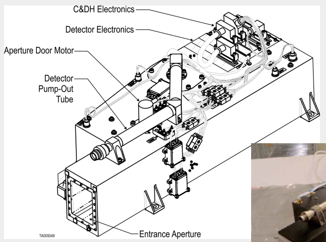

ALICE is a lightweight, low-power spectrograph (750 – 2000 Å) designed for *in situ* imaging spectroscopy of a cometary coma. It operated successfully during the rendezvous with comet 67P/Churyumov-Gerasimenko from August 2014 to the end of mission on September 30, 2016.

Spectral resolution is 8 or 12 Å depending on the position along the 5.5° slit. A spatial pixel (normal to the dispersion) is 0.3° (Stern et al., 2007).

Spectral Signature of O_2 Electron Dissociative Excitation

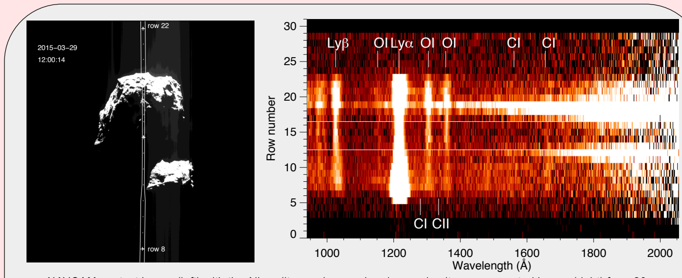

NAVCAM context image (left) with the Alice slit superimposed and near simultaneous spectral image (right) for a 20 minute histogram beginning at UT 11:43 on 2015 March 29. The heliocentric distance was 1.99 AU, the distance to the comet was 92.3 km, and the phase angle was 83.9°. The white horizontal lines outline the 4 rows of the shadowed nucleus used in the spectral extraction. In both images the Sun is towards the top.

Spectrum Extraction and O_2/H_2O Abundance Ratio

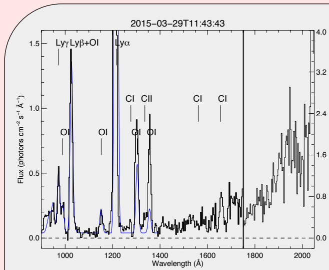

To estimate the abundance of O_2 relative to H_2O along the line of sight above the limb, we assume that the additional brightness of O I λ1356 over that due to electron impact on H_2O is due to electron impact on O_2. We use cross-sections at 100 eV from Makarov et al. (2004) for H_2O and Kanik et al. (2003) for O_2.

$$\frac{N(\mathrm{O_2})}{N(\mathrm{H_2O})} = \frac{B(1356)}{B(Ly\beta)} \times \frac{\sigma(\mathrm{H_2O, Ly}\beta)}{\sigma(\mathrm{O_2, OI\ 1356})}$$

The contribution to OI λ1356 from electron impact on H_2O is evaluated using the relative cross-sections from Makarov et al. and subtracted from the observed OI λ1356 brightness.

$$\frac{\sigma(\mathrm{H_2O, OI\ 1356})}{\sigma(\mathrm{H_2O, Ly}\beta)} = 0.079$$

The strengths of the O I λ1304 and O I λ1356 multiplets suggest abundant O_2. Subtracting an H_2O synthetic spectrum (blue) leaves the λ1356/λ1304 ratio ~2, as expected for electron impact on O_2. The derived abundance ratio of O_2/H_2O = 0.07. This may be an underestimate as Lyman-β is blended with O I λ1026 that can also be excited by e+O_2 (Ajello and Franklin, 1985).

Gas Outbursts

Gas outbursts are characterized by sudden large increases in the atomic emissions from one histogram to the next (5 or 10 minutes), particularly OI λ1356, without a corresponding enhancement in long wavelength solar reflected light characteristic of dust production. Dates in red are from Feldman et al. (2016)

Date (UT)	Peak Time (UT)*a*	r_h (AU)	d (km)	Sub-spacecraft Longitude (deg)	Sub-spacecraft Latitude (deg)	Phase angle (deg)	Local Time	B_max (OI 1356) (rayleighs)*b*
2/27/15	8:30:00	2.22	101	195.8	49.2	59.4	07:30	53
3/21/15	18:57:17	2.05	82	169.5	-27.9	54.8	14:15	21
3/23/15	3:39:56	2.04	79	271.3	-43.5	59.3	12:13	38
4/15/15	9:15:44	1.86	165	249.3	-24.4	72.3	07:36	80
4/15/15	14:05:01	1.86	158	102.4	-22.5	71.4	07:36	50
4/27/15	1:21:36	1.77	116	198.2	-4.8	70.4	16:39	30
4/28/15	3:13:01	1.76	148	166.5	-18.9	75.0	16:49	175
4/29/15	15:47:37	1.75	165	184.5	-30.9	74.9	16:38	65
4/29/15	19:33:36	1.75	160	74.6	-32.1	74.1	16:33	70
4/29/15	23:03:53	1.75	157	332.0	-33.3	73.3	16:28	70
4/30/15	2:32:41	1.75	153	229.3	-34.5	72.5	16:22	70
5/13/15	22:50:55	1.65	158	203.8	55.7	75.1	07:58	75
5/23/15	12:42:22	1.58	143	151.2	-17.1	61.1	16:05	220
6/7/15	19:08:37	1.48	206	191.4	-12.9	87.2	06:00	80
6/8/15	1:22:25	1.48	208	11.3	-10.4	87.4	06:01	72
6/17/15	19:42:02	1.42	212	92.3	56.1	89.9	07:56	105
6/18/15	3:55:15	1.42	202	214.8	51.3	89.9	07:37	160
6/20/15	15:26:15	1.40	181	269.3	19.9	89.9	06:31	60
6/23/15	20:39:02	1.39	196	215.0	53.3	89.7	08:09	110
7/4/15	8:56:47	1.34	179	111.6	53.8	89.9	08:59	95
7/13/15	1:16:13	1.30	155	149.3	15.6	88.8	06:46	85
10/6/15	0:46:29	1.41	764	150.4	-41.0	56.5	06:35	190
10/6/15	2:29:17	1.41	756	99.9	-40.6	56.7	06:36	130
11/7/15	17:32:15	1.61	231	302.9	-1.5	62.6	08:09	60
11/27/15	6:11:02	1.76	126	9.1	-5.1	90.0	05:49	25
12/17/15	19:15:11	1.91	96	81.4	-15.8	89.8	05:36	70
1/1/16	6:00:18	2.02	82	32.9	-51.7	89.3	19:24	58
1/2/16	7:33:02	2.03	88	13.3	-67.1	89.7	20:52	40
1/2/16	12:59:09	2.03	86	217.0	-69.2	89.6	21:15	31
1/2/16	19:07:30	2.03	84	42.5	-71.6	89.4	21:49	45

a) start time of histogram integration and corresponding parameters
b) maximum OI 1356 brightness above the sunward limb

O_2 Driven Outburst on UT 2015 May 23 12:42

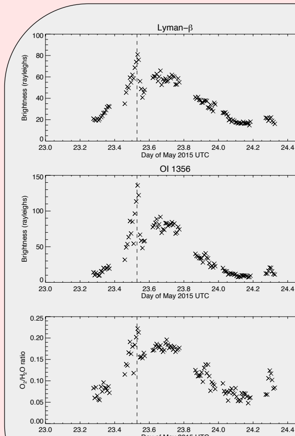

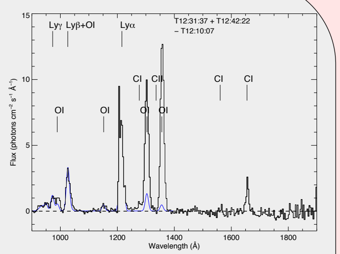

The difference spectrum is characterized by an enhancement in the atomic emissions, particularly atomic oxygen, without a corresponding enhancement in long wavelength solar reflected light characteristic of dust production. The large increase in OI λ1356/OI λ1304 suggests O_2 as the primary source of the additional gas. For the added gas, $N(O_2)/N(H_2O)$ = 0.53. The quiescent value is in the range of 1-10% reported by Bieler et al. (2015) from ROSINA data. While their result for the mean abundance ratio of 3.80 ± 0.85 is often quoted it should be noted that large non-systematic fluctuations were observed during the period between September 2014 and March 2015.

Long-term Behavior

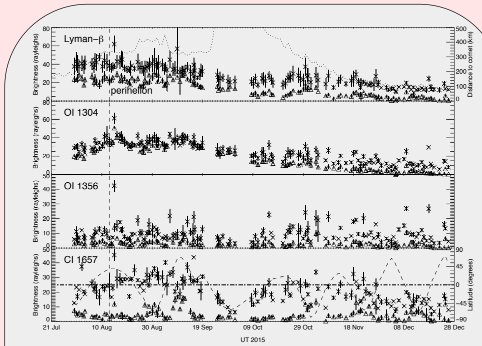

To investigate the long term variability of O_2 in the coma, we utilize a series of ~half-hour exposures taken during "maintenance" nadir pointings between the end of July 2015 and January 2016 on a roughly one day cadence. In each panel above we take the brightness of two spatial rows, both sunward (x) and anti-sunward (Δ) of the nucleus. Enhancements in OI λ1356 are indicative of elevated abundance of O_2 relative to H_2O. The CME event of 2015 October 6 described by Noonan et al. (2018) is off-scale in these plots. The brightening on 2015 August 14, the day after perihelion, is examined in the next panel.

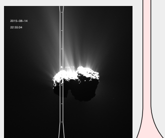

OSIRIS NAC image

2015 August 14-16

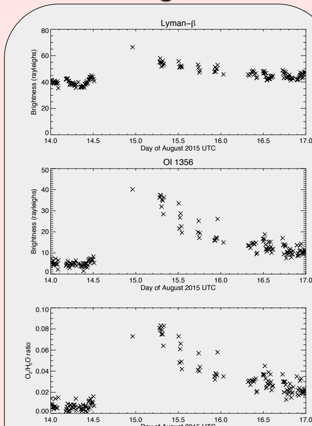

A more detailed light curve for the August 14 enhanced emission, obtained using all of the Alice sunward limb observations over a three day period, shows the slow variation in relative O_2 abundance in the coma.

Discussion and Summary

We initially focused on the source of the O_2 detected during gas outbursts which seemed to be incompatible with the warming of sub-surface volatile reservoirs as the comet approaches perihelion. Water ice containing frozen O_2 would reside below the dust mantle and the sublimated O_2, together with some H_2O, would then percolate through the porous mantle and diffuse into the coma taking some of the dust with it. The absence of dust in the outbursts observed by Alice suggests a different scenario. Skorov et al. (2016), seeking to explain a narrow, short-lived dust outburst observed by the OSIRIS imager, have proposed a deepening of a pre-existing fracture that would lead to the exposure of a sub-surface ice layer and a subsequent rapid ejection of gas and dust. Although Skorov et al. considered a model with CO ice, their calculations should also be valid for O_2. A narrow very short-lived dust jet would be missed by the Alice slit, while the high density of the escaping gas would be distributed collisionally throughout the coma. However, these short outbursts cannot account for the longer-term variability seen in the data. We note that we detected O_2, based on electron dissociative excitation, only between the end of February 2015 and January 2016, corresponding to heliocentric distances inside ~2.2 AU.

Since the observed emissions are excited by energetic electrons in the coma, both the brightness of the emissions and their ratios are sensitive to the electron flux energy distribution as derived from Rosetta Plasma Consortium (RPC) measurements (Galand et al., 2016), as well as models of the distribution of flux along the Alice line-of-sight. In our analysis above we made the simplifying assumption of using relative cross sections at 100 eV, taken from laboratory data available in the literature. Calculations of electron impact ionization using RPC data by Heritier et al. (2018) show large variations with time and position in the coma. Since the ionization and dissociative excitation cross-sections have similar energy dependence we expect commensurate behavior of the atomic emissions. This is an area for future work.

Acknowledgements: Rosetta is an ESA mission with contributions from its member states and NASA. The Alice team acknowledges support from NASA's Jet Propulsion Laboratory through contract 1336850 to the Southwest Research Institute.

References

Ajello, J. M., and Franklin, B.1985, J Chem Phys 82, 2519
Bieler, A., et al. 2015, Nature 526, 678
Feldman, P. D., et al. 2016, ApJL 825:L8
Galand, M., et al. 2016, MNRAS 462, S331
Heritier, K. L., et al. 2018, A&A 618, A77
Kanik, I., et al. 2003, JGR 108, 5126
Makarov, O. P., et al. 2004, JGR 109, 9303
Noonan, J. W., et al. 2018, AJ 156:16
Skorov, Yu. V., et al. 2016, A&A 593, A76
Stern, S. A., et al. 2007, Space Science Reviews 128, 507